ELSEVIER

Catalysis Today 39 (1998) 263–269

CATALYSIS TODAY

New developments in NEXAFS/EXAFS theory

J.J. Rehr*, A. Ankudinov, S.I. Zabinsky

Department of Physics, University of Washington, Seattle, WA 98195-1560, USA

Abstract

Recent advances in the theory of X-ray absorption fine structure (XAFS) are reviewed. Modern ab initio multiple-scattering (MS) calculations now provide an accurate, unified treatment of XAFS, encompassing both EXAFS (extended-XAFS), NEXAFS (near-edge XAFS) and XANES (X-ray absorption near-edge structure). Combined with multi-path analysis techniques, such calculations now permit accurate structural determinations well beyond the first near-neighbor. These calculations also describe near-edge features such as σ^* shape resonances and white lines. Implications for catalyst research are briefly discussed. © 1998 Elsevier Science B.V.

Keywords: EXAFS; NEXAFS; Multiple-scattering; FEFF

1. Introduction

In recent years advances both in theory and analysis methods have revolutionized the technique of extended X-ray absorption fine structure (EXAFS) for local structure determinations [1]. EXAFS refers to the oscillatory structure in the X-ray absorption coefficient beyond about 50 eV of threshold, where the photoelectron backscattering responsible for this phenomenon is relatively weak. EXAFS analysis is no longer limited to first neighbors, and distance determinations are now often comparable in accuracy to those from X-ray diffraction measurements. Significant progress in understanding the near-edge X-ray absorption fine structure (NEXAFS) has also been made. NEXAFS refers to fine structure, such as σ^* shape resonances, in the continuum within about 50 eV of threshold where strong multiple-scattering contributions can be important. Curved-wave multiple-scattering (MS) theory now provides a unified treatment of both EXAFS and near-edge structure, hence the simplified term X-ray absorption fine structure (XAFS) [2]. Often a high-order MS treatment can also describe the X-ray absorption near-edge structure (XANES), i.e., the often intense features within about 10 eV of threshold, such as ''white lines'', which are due to peaks in the local density of states. In this paper we review these advances. In particular we discuss modern MS calculation methods, and the information content in XAFS, by concentrating on the main results with a minimum of technical detail. We also briefly comment on the applicability of the technique to catalysis studies, and refer the reader to more comprehensive reviews, e.g., [3] for further details and references.

The first quantitative calculations of EXAFS were carried out in the 1970s [4], following the pioneering theoretical work of Lee and Pendry [5] and others. For several years thereafter, theoretical calculations for EXAFS analysis were based on the plane-wave

*Corresponding author.

PII S0920-5861(97)00109-0

approximation (PWA) with tabulated scattering amplitudes and phase shifts. These approximations often gave results inferior to those obtained from empirical ''standards''. Moreover, due to the importance of MS corrections, results beyond the first coordination shell were often unreliable. All this has changed dramatically in recent years. Together with modern synchrotron radiation sources and a number of key theoretical developments, the technique of XAFS is now both competitive with and complementary to other high precision structural methods such as X-ray diffraction (XRD). For some complex and disordered materials, XAFS is the superior method for local structural determinations, and is therefore of particular importance for catalyst studies.

Recent theoretical developments have led to a fast high-order MS approach for XAFS calculations in arbitrary systems. In particular we have found that XAFS at all energies is well described by a path-by-path MS approach, with a limited number – typically of order 10^2 – of important paths. Our discussion here reviews these results, but is not meant to be a comprehensive review; details are described in a recent series of papers devoted to XAFS theory [2,6,7]. This approach has been incorporated into efficient ab initio codes FEFF that now include XANES calculations with full elliptical polarization dependence (FEFF version 6) [2]. These codes are highly automated and intended to be ''user friendly'', requiring a minimum of input and thus ensuring reliable results. In parallel developments, new EXAFS analysis procedures have been devised which are compatible with this MS path approach. These include novel automated background removal methods [8] and new fitting codes [9,10] which permit refinement of structural parameters from the MS path data. FEFF has also been adapted for studies of diffraction anomalous fine structure (DAFS) [11] and X-ray magnetic circular dichroism (XMCD) [12] and similar techniques can be used in photoelectron diffraction (XPD) [13].

2. Unified MS XAFS, NEXAFS and XANES calculations

It suffices to give here only a brief overview of the basic formulae, as the MS theory of XAFS [5,6] is now well established. Thus we concentrate in this paper on the key theoretical developments that make modern theoretical calculations possible. The normalized XAFS is defined as $\chi=(\mu-\mu_0)/\mu_0$, where μ is the X-ray absorption coefficient for a given X-ray energy E and polarization $\tilde{\epsilon}$, and μ_0 is the smooth atomic-like background (see our paper [4] for a more detailed discussion). Formally, the calculation of μ is given by Fermi's golden rule

$$\mu(\hat{\epsilon}) \sim \sum_f |\langle c|\hat{\epsilon}\cdot\mathbf{r}|f\rangle|^2 \delta(E-E_f), \tag{1}$$

where $E=\hbar\omega-E_c$ is the photoelectron energy, $\tilde{\epsilon}$ is the X-ray polarization vector, and the sum is over unoccupied final states calculated in the presence of the core-hole. Instead of calculating final states, which is a computational bottleneck, it is equivalent and much faster to reexpress the equation for μ in terms of the photoelectron Green's function or propagator $G(E)$. In turn $G(E)$ can be reexpressed formally as a sum over all MS paths that the photoelectron can take away from the absorbing atom and back [5]. When carried to all orders (full MS), this theory is equivalent to ''exact'' treatments. For example, for a small cluster, the sum can be taken to all orders by matrix inversion. However, due to the large dimension of the matrix, such calculations are computationally intractable beyond 50–100 eV of the absorption edge [15,16].

2.1. Curved-wave scattering theory

One of the key theoretical developments is an efficient curved-wave scattering theory. Due to curved-wave effects, exact calculations of MS contributions are time-consuming and have only been carried out for a few low-order MS paths [17]. To overcome this bottleneck, we have devised an efficient method for curved-wave MS calculations based on the Rehr–Albers (RA) scattering matrix formalism [6]. The main idea behind the RA approach is a separable representation of the two-center Green's function propagator, which leads to great computational efficiency. The approach yields an accurate expression analogous to the standard XAFS equation for the contribution to the XAFS from each MS path Γ:

$$\chi_\Gamma(E) = S_0^2(E) N \frac{|f_{\rm eff}(k)|}{kR^2} \times \sin(2kR + 2\delta_c + \Phi) e^{-2R/\lambda_e - 2\sigma^2 k^2}. \tag{2}$$

Here, $f_{\rm eff}(k)=|f_{\rm eff}(k)|e^{i\phi}$ is the effective curved-wave scattering amplitude (from which FEFF is named), δ_c is the real part of the final state l-wave central-atom phase shift, $k=[2(E-E_F)]^{1/2}$ is the wave number measured from threshold E_F, λ is the XAFS mean-free path, σ is the r.m.s. fluctuation in the effective path length $R=R_{\rm path}/2$, and $S_0^2(E)$ is a factor near unity that takes into account many-body loss effects.

With the RA approach, we have shown that the *effective scattering amplitude* $f_{\rm eff}$ can be expressed accurately as a product of low-order (typically 6×6) matrices F. For single scattering the result is exact. For example, for an N-leg path Γ with scatterers at $\boldsymbol{R}_1, \boldsymbol{R}_2, \ldots, \boldsymbol{R}_N$ we obtain

$$f_{\rm eff} = \frac{kR^2}{\rho_1\rho_2\cdots\rho_N}\,{\rm Tr}\,MF^N\cdots F^2F^1. \tag{3}$$

This formula is analogous to the one from the PWA, except that the factors are matrices instead of scattering amplitudes. However, due to curved-wave effects, the net result differs greatly from the PWA, even at the highest photoelectron energies ($\sim$100 eV). Here $\boldsymbol{\rho}_i=p(\boldsymbol{R}_i-\boldsymbol{R}_{i-1})$, $p=[2(E-V_{\rm mt})]^{1/2}$ is the complex photoelectron momentum measured with respect to the muffin-tin zero, F^i is the RA scattering matrix at site i, and M is the $l=1$ termination matrix.

2.2. Path filters

Another computational bottleneck is the number of paths needed to be calculated, since this number proliferates exponentially with increasing path length. To overcome this bottleneck, we have devised an efficient constructive algorithm for enumerating the most important MS paths in the calculations [2]. In particular we restricted the number of paths by introducing ''filters'' in the path enumeration scheme. We have found that the majority of MS paths are numerically insignificant or tend to cancel one another due to random phase incoherence, and that the most important paths tend to be linear and triangular. To automate the path selection procedure, the contribution of a given MS path was roughly estimated using the PWA, and only those paths of amplitude larger than a given cutoff were retained. To speed the calculation, physically equivalent paths are hash-sorted, and then calculated accurately only once. With such filters typically only a few hundred distinguishable MS paths ever need to be calculated to yield XAFS accurate to within experimental accuracy of a few percent.

2.3. Scattering potentials

Another key theoretical development is an efficient and accurate approximation for the scattering potentials. The considerations in constructing such potentials are quite different from ground state electronic structure or quantum chemistry calculations. Scattering by electrons of moderate energy depends largely on the potential and density in the core of an atom, where the muffin-tin approximation and spherical symmetry are both good approximations. Moreover, the electron density there is well described by a relativistic overlapped SCF atomic charge density or Matheiss prescription. Also an automated prescription for construction of the muffin-tin radii is available. Relativity is needed for the core atomic charge density but for photoelectron energies of order 1000 eV or less, a non-relativistic scattering description is adequate. Details of the muffin-tin scattering potential and scattering phase shifts used in FEFF are given in [7].

2.4. Self-energy

A crucial difference between ground state electronic structure calculations and XAFS is the need for an energy dependent ''self-energy $\Sigma(E)$''. This quantity is the analog of the more familiar exchange–correlation potential $V_{\rm xc}$ in density functional theory. In fact, we have found that the self-energy is often more important than self-consistency [7]. FEFF uses an efficient calculation of the complex Hedin–Lundqvist self-energy, modified to include low-energy electron–hole losses. This self-energy model builds in inelastic losses automatically and has been found to give good agreement for electron mean-free paths at high energies, as determined by experiment, and thus avoids the need for ad hoc mean-free path terms. Secondly, the scattering potential needed is that for the final state in the presence of a (usually fully relaxed) core-hole, in accordance with the final state rule. Details of our self-energy prescription are given in [7].

2.5. Thermal and configurational disorder

Yet another key theoretical development is the cumulant expansion for including thermal and configurational disorder in bond lengths [18]. One of the least satisfactory aspects of full MS treatments is the neglect or crude treatment of disorder. However, such effects can be included straightforwardly in path-by-path methods. FEFF only treats the mean square variation σ^{2_T} (the dominant term) in the net half path length, and ignores angular variations, which can be added in fitting schemes. For small displacements, this gives a Debye–Waller factor, $W = \exp(-2\sigma_T^2 k^2)$ for each MS path. As a rough approximation, the thermal contributions to the Debye–Waller factor may be approximated by an isotropic Debye model [19] with a single parameter – the Debye-temperature Θ_D – which is a useful measure of local bond strength. As a consequence the MS Debye–Waller factors contribute significantly to the convergence of the MS expansion. At high temperatures or for large structural disorder, the Debye–Waller factor is complex valued and thus affects the XAFS phase. W can be expressed most simply using the cumulant expansion [18,20],

$$W(k) = -\sum_n (2ik)^n \frac{\sigma^{(n)}}{n!} = 2k^2\sigma^2 + \frac{4}{3}ik^3\sigma^{(3)} - \frac{2}{3}k^4\sigma^{(4)} + \cdots \quad (4)$$

The third cumulant $\sigma^{(3)}$ characterizes the anharmonicity or asymmetry in the pair distribution function. If not taken into account in the analysis, it causes bond distances to appear shorter and the wrong temperature dependence. These corrections can be very important in disordered materials especially at high temperature and are often important in catalyst studies.

3. Applications to XAFS, NEXAFS and XANES

Following the introduction of the new theoretical methods outlined above, complementary MS analysis techniques have been developed [1]. With such techniques an analysis well beyond the first coordination shell is now possible. MS XAFS analysis packages that make use of the phase and amplitude data in the FEFF codes have been developed by several groups. These include, e.g., FEFFIT [9], a part of the University of Washington analysis package UWXAFS (version 2), and EXAFSPAK [10], an analysis package developed at Stanford Synchrotron Radiation (SSRL).

3.1. Information content in XAFS

The utility of XAFS as a structural analysis technique depends on an accurate knowledge of the phase shifts and scattering amplitudes in the XAFS formula. Presently these are known to sufficient accuracy to determine distances to about 0.01 Å and coordination numbers to about ±1. To illustrate this, we show in Fig. 1 the Fourier transform of the XAFS of fcc Pt metal, phase corrected by the theoretical first shell XAFS phase, $2\delta_c+\Phi$ [21]. Note that all peaks in this transform are centered near the correct crystallographic near-neighbor distances: 2.78, 3.93, 4.81, 5.56 Å, ..., respectively. Because the XAFS phase shift is usually dominated by the central-atom contribution $2\delta_c$, we argue that the use of such phase-corrected Fourier transforms can be visually advantageous (i.e., single-scattering peaks will appear sharper). This will be true even for disordered systems with more than one type of atom in the first coordination shell. However, fits are not significantly affected by the type of transform used. In structural refinements, one can assume that f_{eff} is insensitive to small variations in near-neighbor distances. The number of independent structural parameters that can be determined by XAFS, is given by a phase-

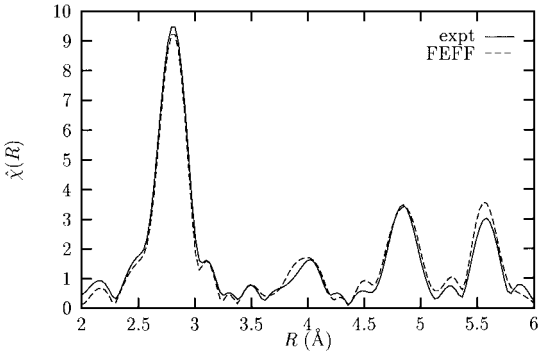

Fig. 1. Phase-corrected k^2 weighted Fourier transform of Pt L3 XAFS calculated by FEFF (dashed lines) and compared to experiment at 80 K (solid lines).

space counting argument in signal theory, as discussed by Kincaid et al. [22], $N=(2/\pi)\Delta k\Delta R$, where Δk is the range of the data and ΔR is the range in the r-space transform of $\chi(k)$ covered by a given shell. For example, for Pt, the number of structural parameters that can be fit by data over the k range from 2 to 19 Å^{-1} and the r range [3.5–4.5] of the second shell and 111 triangle paths is approximately 9, which is sufficient to determine distances, amplitudes and a few angles.

3.2. NEXAFS and XANES

An excellent treatise on NEXAFS is given by Stohr [23]. As a prototypical example of NEXAFS, we review the polarization dependence of the diatomic molecule N_2 using high-order MS calculations [7]. This calculation provides a strong test of MS theories because of the short bond length and strong low-energy scattering in low-Z atoms. A primary goal of our original study was to understand the σ^* shape resonances [23], which are of much interest in surface and catalyst studies since their peak locations in energy are correlated with bond length [24]. Indeed, we have shown that the shape resonances in O_2 and N_2 can be explained quite simply by successive MS contributions from repeated bounces between the two scattering sites. Here, we only illustrate these results, together with their polarization dependence. By taking advantage of the p-wave ''search-light'' effect, polarization can be used to determine the orientation of a molecule on a surface, as well as its bond distance, as shown in Fig. 2 for N_2. We found that the large backscattering amplitude and the coherence of the MS phases control the resonance, and give a generalization of the Natoli rule [24] relating peak position with bond length. In particular, we find that the local momentum (defined relative to V_{mt}) at the peak is

$$p = \frac{m\pi - \Delta\Phi}{R}, \tag{5}$$

where R is the near-neighbor bond length and $\Delta\Phi$ is the difference in the XAFS phase between n and $n+1$ backscatterings [7]. We have found that this formula also explains well the variation with peak position and bond length in C_2H_2, C_2H_4, and C_2H_6 [23]. However, in materials with more than one strong bond (e.g., graphite), the results are more difficult to interpret. We have also found that the height of the shape resonances is sensitive to temperature, due to the strong exponential decay of high-order terms, which vary as $\exp[-n^2\sigma^2p^2/2]$. This illustrates how the Debye–Waller factors can control the convergence of the MS series.

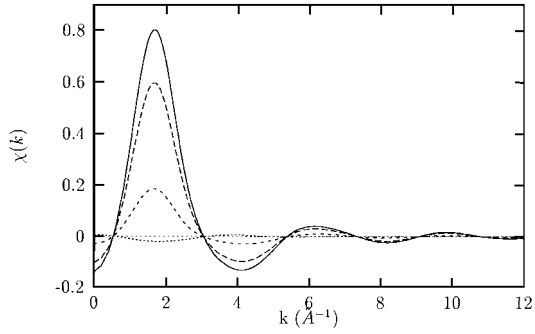

Fig. 2. σ^* shape resonance and NEXAFS structure in N_2 vs. polarization angle with respect to the molecular axis from FEFF6: 0° (solid), 30° (dashes), 60° (short dashes), and 90° (dots).

3.3. XANES

''White lines'' are striking features in XANES which are due to strong peaks in the unoccupied densities of states near threshold. Since its near edge has a strong white line just above threshold [2], Pt metal provides an important test case for XANES calculations. We use the analogous term ''black line'' to describe the corresponding dip in intensity at the edge seen in many other spectra, e.g., Cu K-shell XANES. As in XAFS, the XANES spectra can be obtained from the relation $\mu=\mu_0(1+\chi)$, where μ_0 is the background absorption and χ the polarization averaged XAFS. We have found that the theoretical XANES structure are in reasonable agreement with the experiment. In particular the white line is adequately reproduced by the theory [2]. Moreover, the theory correctly accounts for all the peaks in the experimental spectrum, except for slight errors in peak locations and amplitudes. Strikingly, we have found that the presence of a core-hole is a crucial ingredient in the calculations, in agreement with the final state rule. The non-monotonic behavior in $\mu_0(E)$ beyond the white line also illustrates the importance of atomic-XAFS [14].

4. Applications to catalysis studies

The importance of XAFS in catalysis studies has been recognized for many years [25]. For modern examples, see the comprehensive series of reviews in [3] or the section on catalysis in the Proceedings of the International Conference on XAFS and XANES [1], and references therein. Since XAFS is well suited for studies of dilute and highly disordered materials, the method is an excellent approach for the study of practical, highly dispersed catalysts and their morphology, as well as metal-support interactions [26]. It has been shown, e.g., that the XAFS is quite sensitive to the size dependence of small metal clusters and coordination numbers can be used to quantify cluster size and shape [26]. Larger clusters naturally exhibit sharper XAFS features (i.e., higher frequency components) due to the presence of longer paths. Moreover, it has recently been shown, using both the FEFF6 [2] and CONTINUUM [16] codes, that the near-edge structure is also sensitive to cluster size [27]. The effects of oxidation and reduction are also visible, e.g., through the comparison of the number of metal–metal and metal–oxygen bonds, although it is still difficult to quantify charge transfer precisely. Thus with the modern theoretical codes and analysis tools now in hand, XAFS studies are providing increasingly more accurate detail concerning the structure and nature of catalysts.

5. Conclusions

The FEFF codes now make possible a general high-order polarized-MS treatment of XAFS, NEXAFS and XANES. Accurate automated scattering potentials, self-energies and Debye–Waller factors are essential for the success of these codes. The accuracy of our MS calculations permits more definitive conclusions concerning interatomic distances and disorder than had previously been possible with the XAFS technique. We find that a purely single-scattering interpretation XAFS Fourier transform is not reliable; MS contributions can dominate shadowing paths and are crucial at large distances. For the near edge, MS contributions are essential and even NEXAFS features, such as continuum σ^* shape resonances and XANES features such as white lines are often well described by a high-order MS theory. However the remaining discrepancy between calculated and experimental XANES and NEXAFS amplitudes suggest that further improvements are needed for edge calculations. The accuracy of distances obtained with our codes is usually better than 0.02 Å. Indeed, in another work [28], it has been found that the improved phase shifts used in FEFF have eliminated the discrepancies in distance determinations between SEXAFS and other spectroscopies such as LEED and XPS. The correlated-Debye model is found to be a useful first approximation to vibrational amplitudes and displacement–displacement correlations. The MS contributions to XAFS can be understood quantitatively in terms of a relatively small number (typically of order 100) paths. Single-scattering, triangle, and linear or near-linear paths and path groups are found to be the most important. Moreover, because of the strong interference and coherence between paths within a path group (i.e., a set of paths with closely similar geometry and path lengths), a group of paths can have more or less importance than any individual path within the group. Thus, MS EXAFS calculations can now be considered as well understood.

Acknowledgements

We thank R.C. Albers and J. Mustre de Leon for their valuable assistance in developing the FEFF codes. We also thank D. Sayers and D. Bazin for discussions on modern catalysis studies using XAFS and F. Bridges, M. Newville, B. Ravel and E.A. Stern for discussions on modern XAFS analysis methods. This work was supported in part by the US Department of Energy grant DE-FG06-ER45415-A003.

References

[1] Proceedings of the International Conference on XAFS and XANES, Physica B 208–209 (1995).
[2] S.I. Zabinsky, J.J. Rehr, A. Ankudinov, R.C. Albers, M.J. Eller, Phys. Rev. B 52 (1995) 2995.
[3] Y. Iwasawa (Ed.), X-ray Absorption Fine Structure for Catalysts and Surfaces, World Scientific, Singapore, 1996.
[4] D.C. Konigsberger, R. Prins (Eds.), X-ray Absorption: Principles, Applications, Techniques of EXAFS, SEXAFS and XANES, Wiley, New York, 1988 (and references therein).

[5] P.A. Lee, J.B. Pendry, Phys. Rev. B 11 (1975) 2795.
[6] J.J. Rehr, R.C. Albers, Phys. Rev. B 41 (1990) 8139.
[7] J.J. Rehr, R.C. Albers, S.I. Zabinsky, Phys. Rev. Lett. 69 (1992) 3397; J.J. Rehr, J. Mustre de Leon, S.I. Zabinsky, R.C. Albers, J. Am. Chem. Soc. 113 (1991) 5135.
[8] G.G. Li, F. Bridges, G.S. Brown, Phys. Rev. Lett. 68 (1992) 1609.
[9] M. Newville, B. Ravel, D. Haskel, J.J. Rehr, E.A. Stern, Y. Yacoby, Physica B 208–209 (1995) 154.
[10] G. George, EXAFSPAK, unpublished.
[11] H. Stragier, J.O. Cross, J.J. Rehr, L.B. Sorensen, C.E. Bouldin, J.C. Woicik, Phys. Rev. Lett. 69 (1992) 3064.
[12] A. Ankudinov, J.J. Rehr, Phys. Rev. B 52 (1995) 10214.
[13] C.S. Fadley, in: R.Z. Bachrach (Ed.), Synchrotron Radiation Research: Advances in Surface Science, Plenum Press, New York, 1991; A.P. Kaduwela, D.J. Friedman, C.S. Fadley, J. Electron Spectroscopy Relat. Phenomena 57 (1991) 223.
[14] J.J. Rehr, C. Booth, F. Bridges, S.I. Zabinsky, Phys. Rev. B 49 (1994) 12347.
[15] P.J. Durham, J.B. Pendry, C.H. Hodges, Comput. Phys. Commun. 25 (1982) 193; D.D. Vvedensky, D.K. Saldin, J.B. Pendry, Comput. Phys. Commun. 40 (1986) 421.
[16] C.R. Natoli, D.K. Misemer, S. Doniach, F.W. Kutzler, Phys. Rev. A 22 (1980) 1104.
[17] S.J. Gurman, N. Binsted, I. Ross, J. Phys. C 19 (1986) 1845.
[18] E.D. Crozier, J.J. Rehr, R. Ingalls, in: Proceedings of the International Conference on XAFS and XANES, Physica B 208–209 (1995).
[19] G. Beni, P.M. Platzman, Phys. Rev. B 14 (1976) 9514.
[20] M. Benfatto, C.R. Natoli, A. Filipponi, Phys. Rev. B 40 (1989) 9626.
[21] E.A. Stern, M. Newville, B. Ravel Y. Yacoby, D. Haskel, Physica B 208 & 209 (1995) 117.
[22] P.A. Lee, P.H. Citrin, P. Eisenberger, B.M. Kincaid, Rev. Mod. Phys. 53 (1981) 769.
[23] J. Stöhr, NEXAFS Spectroscopy, Springer, Heidelberg, 1992.
[24] C.R. Natoli, in: A. Bianconi et al. (Eds.), EXAFS and Near Edge Structure, Springer, New York, 1983, p. 43.
[25] F.W. Lytle, P.S.P. Wei, R.B. Greegor, G.H. Via, J.H. Sinfelt, J. Chem. Phys. 70 (1979) 4849.
[26] G.H. Via, J.H. Sinfelt, in: Y. Iwasawa (Ed.), X-ray Absorption Fine Structure for Catalysts and Surfaces, World Scientific, Singapore, 1996, p. 147; Z.C. Zhang, G. Lei, W.M.H. Sachtler, ibid, p. 173; K. Asakura, Y. Iwasawa, ibid, p. 192; B.S. Clausen, H. Topsoe, ibid, p. 235; D.C. Koningsberger, F.B.M. Van Zon, M. Vaarkamp, A. Munoz-Paez, ibid, p. 257.
[27] D. Bazin, D. Sayers, J.J. Rehr, C. Mollet, J. Phys. Chem. B 101 (1997) 5332.
[28] L. Tröger, D. Arvanitis, J. Rehr, T. Lederer, T. Yokohama, K. Baberschke, E. Zscheck, Jpn. J. Appl. Phys. 32 (1993) 137.